Direct Identification of Multilayer Graphene Stacks on Copper by Optical Microscopy

Yu Cheng[†,‡], Yenan Song[†,‡], Dongchen Zhao[†,‡], Xuewei Zhang[†,‡], Peng Wang[†,‡], Miao Wang[§], Yang Xia[¶], Shigeo Maruyama[#], Pei Zhao[†,‡,], Hongtao Wang[†,‡,*]*

[†]Institute of Applied Mechanics and

[‡]Key Laboratory of Soft Machines and Smart Devices of Zhejiang Province

Zhejiang University, Hangzhou 310012, P. R. China

[§]Department of Physics, Zhejiang University

Hangzhou 310012, P. R. China

[¶]Institute of Microelectronics, Chinese Academy of Science

Beijing 100029, P. R. China

[#]Department of Mechanical Engineering, The University of Tokyo

Bunkyo-ku, Tokyo 113-8656, Japan

*Author email: peizhao@zju.edu.cn (Pei Zhao),

htw@zju.edu.cn (Hongtao Wang)

ABSTRACT

Growing graphene on copper (Cu) by chemical vapor deposition (CVD) has emerged as a most promising approach to satisfy its practical requirements, but the fast and large-scale characterization of its grown adlayers remains a challenge. Here we present a facile and inexpensive method to directly identify the multilayer graphene stacks on Cu by optical microscopy, using simple ultraviolet and heating treatments. The sharp optical contrast, originating from the variation in copper oxide thickness underneath graphene, reproduces the stacking geometry with high fidelity to scanning electron microscopy observation, demonstrating the correspondence among the optical contrast, the oxide thickness variation and the stack of adlayers. The close correlation roots in the throttling effect of graphene grain with discrete structural defects in controlling the rate-determined copper oxidizing agent supply. We believe that this approach can enable large-scale evaluation of CVD-derived graphene quality, which are critical for optimizing CVD processing parameters of graphene growth.

Graphene, a new two-dimensional material, has been attracting enormous research interests in various fields over the past decade, due to its excellent mechanical, thermal, and electrical properties.[1-4] Among the different graphene synthesis methods,[5-10] chemical vapor deposition (CVD) on copper (Cu) foils has proven to be the most promising and efficient one to obtain graphene samples with different crystallinity and layer structures up to wafer scale.[7, 11-15] However, as graphene nucleation is a process originated from the carbon (C) super-saturation at the active sites of Cu surface,[16, 17] graphene adlayers are always simultaneously formed during the growth of the monolayer, depending on CVD conditions such as temperature, hydrogen and methane concentration,[18, 19] texture and pre-treatments of Cu substrates.[20, 21] The overall uniformity will be impaired due to the thickness variation in graphene with adlayers, being detrimental to applications of large-scale electronic device integration. By far, it remains a challenge in fast and large-scale characterization of adlayers in a CVD-derived graphene film. Scanning electron microscopy (SEM), Raman spectroscopy, and atomic force microscopy (AFM) are the most widely used techniques. SEM can directly detect the graphene adlayers on Cu based on their number-of-adlayer related secondary electron yields, but the scanning field is limited in scale of millimeters. Raman and AFM characterizations are not applicable to the direct measurements of as-grown graphene adlayers on Cu due to the substrate fluorescence or surface roughness. These measurements demand a polymer-assisted transferring process of graphene from its grown substrate to other flat substrate. For OM characterization, SiO_2 (285 nm in thickness) / Si wafers are usually taken as the flat substrates,[22] on which graphene and its different adlayers are made visible to some wavelength range of visible light owing to the 2.3% absorption per graphene layer and the refraction of the thin SiO_2 film. For the purpose of graphene adlayer detection and uniformity evaluation, graphene transfer is rather time-

consuming and expensive because of the involved Cu-etching process as well as the necessary chemicals and special substrates.[11, 23, 24]

Surface oxidization combined with optical microscopy (OM) provides another approach to directly characterize the uniformity of CVD-derived graphene on its grown substrate of Cu foil without any transferring process. Duong *et al.* found that ultraviolet (UV) light can selectively oxidize Cu underneath graphene grain boundaries, making them visible by conventional OM.[25] Oxidation creates structural defects in graphene with the help of Cu catalysis, emerging as a new microscopic method to probe graphene layers. Gan *et al.* recently developed a technique to directly visualize the second layer of graphene on Cu using OM, by employing an ambient-condition heating process to remove the top graphene monolayer.[26] However, no graphene multilayers beyond bilayers can be probed by this method.

Here we present a facile and inexpensive method to directly identify multilayer graphene stacks on Cu by OM, using simple UV treatment followed by heating at ambient conditions. The sharp optical contrast, originating from the variation in copper oxide thickness underneath graphene grains, reproduces the stacking geometry with high fidelity to the SEM observation of the pristine samples, demonstrating the correspondence among the optical contrast, the copper oxide thickness variation and the number and stack of adlayers. The close correlation roots in the throttling effect of graphene grain with discrete structural defects in controlling the rate-determined copper oxidizing agent supply.

RESULTS

Oxygen-assisted CVD developed by Hao *et al.* provides a method to obtain large-scale graphene single crystals by suppressing the active sites on Cu for graphene nucleation.[14] We

adopted this method to synthesize the pristine graphene samples with typical grain sizes range from 0.5 to 1 mm. The visualization procedure simply consists a two-step treatment, as schemed in Figure 1a. Pristine graphene single crystals, which have no color contrast, are firstly exposed in the UV light for 3 hours using a common UV lamp with power output of 20 $\mu W \cdot m^{-2}$, followed by heated on a hot plate at 300 ºC in air. The UV treatment duration can be greatly reduced by increasing the light intensity. For clarity, pristine graphene is illustrated with a slight color difference from the Cu substrate in Figure 1a(i). After oxidation, a set of six-fold patterns with star-like or hexagonal shapes with strong color contrast is observed by OM (Figure 1b), which reproduces the geometry of graphene adlayer stack within this graphene single crystal observed by SEM in the same region (Figure 1c). The second (2L), third (3L), fourth (4L) and fifth (5L) layers from the outermost to the innermost can be clearly identified, and the overview of the much larger-sized graphene first layer (1L) is shown in Figure S1 in Supplementary Information. These consistent observations between the oxidation/OM and SEM demonstrate the practicability of this new method for the direct identification of different graphene adlayers on Cu surface.

The processing time of UV and/or heating is varied in order to clarify the factors that affect graphene adlayer visualization. Figure 2 compares the dependence of visualized graphene layer number on the UV treatment time of 60 min, 120 min and 150 min followed by fixed-time ambient heating for 30 s. Consequently, the 2L, 3L and 4L of graphene adlayers can be distinguished with prolonged UV-treatment time. The corresponding SEM images of the same graphene grains prove that they actually contain more graphene adlayers with at least four layers, as shown in Figure 2d-f. This demonstrates that the extent of graphene adlayers that can be

visualized is strongly dependent on the time of UV treatment, and longer time of UV exposure helps visualize graphene adlayers with more layer numbers.

Figure 3 compares the OM images of graphene grains after UV exposure with and without ambient-condition heating. With no heating treatment, the outline of the second and up to the third adlayer can be discernible by OM after the UV-light exposure for 150 min (Figure 3c) or even longer time. The contrast among different number of adlayers are relatively weak with only UV treatment, suggesting less severe oxidation to the Cu substrate. This contrast can be significantly enhanced by 30 s ambient-condition heating at 300 ºC (Figure 3d-e). As discussed later, the grey scale of the contrast is closely related to the thickness of the copper oxide. Furthermore, the 3L and 4L are visible at the center areas of graphene grains with pre-UV treatment for 120 min and 150 min, respectively, which are invisible with only the UV treatment. For all the graphene grains shown in the OM images of Figure 3, the center adlayers are displayed in a bright color and the surrounding adlayers are relatively darker. This color difference suggests less oxidation of the center region due to the better protection from oxygen attacking with increased number of graphene adlayers. It is noted that a longer heating process will reduce the color contrast from different number of graphene adlayers (Figure S2 in Supplementary Information). Optimized processing time highly depends on the heating temperatures, ranging from 10 s (300 ºC) to 12 min (200 ºC) in order to maximize the contrast for identifying geometries of at least 4L graphene adlayer stacks (Figure S3 in Supplementary Information), given a fixed UV exposure. Figure 3g summarizes the effect of the time of UV treatment and heating on the adlayer layer visualization. Without heating, up to 3L graphene adlayer can be visualized by UV exposure regardless of its treating time. A followed 10 s ambient-condition heating render more pronounced effect of the same UV treatment, as

exemplified by visualizing hexalayer graphene stacks with a common UV lamp (Figure S4 in Supplementary Information), *e.g.* a low-pressure Hg light with power output of 20 $\mu W \cdot m^{-2}$ and majority light at a wavelength of 254 nm. Such post short-time ambient-condition heating process is critical in enhancing the optical contrast so as to realize the visualization.

The optical contrast of stack graphene adlayers comes from the different underneath copper oxide thickness. Figure 4a plots the height contour of a graphene single crystal area with stacking adlayers after 3 h UV exposure followed by 30 s ambient-condition heating treatment. The height profile along the dashed line in Figure 4a presents a clear tendency of decreased height from 5L to 1L. The abrupt height difference across the boundaries of adjacent adlayer regions is in the order of tens of nanometers. Considering that the thickness of a graphene monolayer is only 0.34 nm,[27] such difference in heights of adjacent adlayers is the manifestation of the thickness variation of the underneath copper oxide (Cu_xO) due to oxidization by both UV and heating treatments. The existence of the Cu_xO layer can also be supported by OM imaging using light with different wavelengths. Since the reflectance of a Cu_xO layer is strongly related with its thickness and the light wavelength,[28] the oxidized graphene samples take different optical contrast when observed using light with different wavelengths. Figure 4b and c compare the OM images of the same graphene area but observed using yellow and blue light, respectively. Regardless of the overall background color for the images, the adlayers in the same graphene grain exhibit different contrast for varied layers when shined by yellow or blue light. This observation confirms the assumption that the contrast of graphene adlayers originates from the different reflectance of Cu_xO layer with varied thicknesses. The reduction-oxidation experiments on the oxidized graphene sample is consistent with the above observation as well (Figure 4d-e). A mild reduction of oxidized graphene by acetic acid fully smear out the color contrast of its

adlayers. A re-heating treatment to this sample easily brings the color contrast back to its original state, as shown in Figure 4d-e. Most importantly, the height contour (Figure 4a) reproduces the pentalayer graphene stack geometry with high fidelity to the OM image of the same region (Figure 4b-c), directly demonstrating the correspondence among the optical contrast, the copper oxide thickness variation and the number of adlayers.

The oxidation of the underneath Cu substrate requires diffusion of oxygen species through the stack graphene adlayers. It is expected that the structural modification to graphene by UV or heating treatments plays a key role in enabling visualization of the number of adlayers by OM. Confocal Raman spectroscopy was employed to characterize the different pristine and oxidized graphene samples. All samples were transferred to Si/SiO_2 substrate in order to avoid strong fluorescence from Cu substrates. Raman spectra from a non-treated graphene grain (Figure 5a) exhibited clear and well-defined fingerprints of areas that contain different number of layers, such as G-bands with different intensities, 2D-bands with different band positions and full-width-at-half-maximum (FWHM) values, as well as the varied ratios between the G- and 2D-bands (2D/G ratio).[29] These Raman spectrum features are consistent with the layer numbers measured by the SEM images. Moreover, for all different layers in pristine graphene, the Raman spectra of the adlayers show negligible D-band (Figure 5a), indicating the overall high quality across this sample. No significant difference in Raman spectra was observed between pristine and ambient-condition heated graphene samples (Figure 5b), except appearance of a small D band in the graphene monolayer after a short time ambient heating at 300 ºC. In contrast, the prolonged UV treatment induces more structural defects. Apparent D-bands emerge for all the Raman spectra of graphene with different layer numbers after a 3-hour UV treatment (Figure 5c), which indicates quality reduction due to the UV-generated structural defects. Especially, the D-

band intensity is higher than that of the G-band for the Raman spectrum of 1L graphene. The D-band to G-band ratio (D/G ratio) is approximately 1.3. This ratio decreases with increasing number of graphene layers, suggesting a reduction of the average density of UV-generated defects. A synergetic effect has been observed if graphene grains are treated by a short-time ambient heating after UV exposure. Much higher D-bands show up in Raman spectra of all stack graphene adlayers (Figure 5d). Theoretical results show that oxygen etching of the edge atoms in grain has an activation energy of approximately 1.1 eV,[30] and with the unrestricted access of oxygen from the exposed Cu to the graphene edge, it is possible to lower this oxidation resistance and destruct monolayer graphene areas that are in contact with Cu surface by expanding from the edges of the defects or cracks, as demonstrated by Gan *et al.*.[26] However, this oxygen etching process only precisely occurs to the monolayer areas but not the multilayers.[26] This can also be confirmed by the D-bands that only observable in the 1L graphene but not the others. On the other hand, when UV treatment is solely adopted, the oxygen atoms can bond effectively to the C atoms of the graphene, with an activation energy of 5.6 eV.[31] The oxidation process can further lead to the release of CO or CO_2 molecules,[31] resulting in the formation and expansion of surface vacancies in all different layers, which provides additional graphene edges for the followed oxygen etching process of these layers by the ambient-condition heating treatment. It is therefore expected that abundant oxygen molecules in air react more easily with sites containing non-sp^2 bonds at elevated temperatures, which explains that the ambient heating causes fast structural destruction of defective graphene (Figure 5e). On the other hand, the UV treatment induces discrete defects for both the low chemical reaction selectivity and the low concentration of reactive oxygen species (Figure 5f).

DISCUSSION

Previous studies have shown that low temperature copper oxidation (T < 300 ºC) leads to formation a uniform film of Cu_2O or Cu_3O_2 in the early stage (< 10 min).[32] The oxide film is porous with thickness less than a few hundred nanometers. The fast diffusion of ambient oxygen through a porous thin oxide film renders that the oxidation kinetics in this step is solely determined by the low-temperature chemical reaction on the Cu_xO/Cu interface when a Cu foil is heated in air at 300 ºC. Different scenario will be expected if the Cu surface is fully isolated from oxygen molecules by conformally covered pristine graphene (Figure 6i). In between the two limiting cases, a graphene grain with discrete structural defects may act a throttle in controlling the oxidizing agent supply. Room temperature UV exposure in air is a facile and easily available method to mildly induce defects into graphene grains without causing structure destruction, as shown by Raman spectroscopy (Figure 5c). During UV treatments, a small amount of ground state $O(^3P)$ atoms and ozone (O_3) molecules are generated

$$O_2 + h\nu = 2O(^3P)$$

$$O(^3P) + O_2 = O_3$$

O_3 is only physisorbed on graphene surface, while $O(^3P)$ is absorbed on the bridge site of the C hexagons to form an epoxy group, which can further induce vacancies into the topmost layer by removing carbon atoms together with their bonded oxygen epoxide groups.[31, 33, 34] These vacancies expose the second topmost layer to the UV/$O(^3P)$ environment, leading to a similar process of C atom removal. This process can be extended to the most inner graphene adlayers, given enough UV/$O(^3P)$ exposure. The effect of UV treatment is schematically shown in Figure 6ii. Meanwhile, the Cu surface underneath the defective few-layer graphene will also be

oxidized by $O(^3P)$ (Figure 6iii), appearing optical contrast with layer number. However, the low concentration of $O(^3P)$ greatly limits the growth of Cu_xO, rendering very poor optical contrast (Figure 3a-c). Only 1L, 2L and 3L regions can be identified by exclusive UV treatments. The contrast enhancement is realized after ambient condition heating treatment. At 300 ºC, Cu_xO almost instantaneously forms when oxygen molecule reaches Cu surface by diffusing through the UV-generated vacancy channels in stack graphene adlayers. Fewer channels are available in thicker graphene layers, rendering differential oxygen supply and consequently variation in copper oxide thickness. This process is outlined in Figure 6iv. It is noted that optimized UV treatment time will maximize the difference in the throttling effect of stack graphene adlayers, which determines number of adlayers can be identified in combined with ambient heating (See summary in Figure 3g). On the other hand, a prolonged heating at 300 ºC will finally smear out the optical contrast in different regions due to the severe oxidation of defective graphene as revealed by Raman spectroscopy (Figure 5d). Therefore, we adopt a low temperature of 300 ºC and a short time of less than 30 s to maximize the optical contrast. Under this condition, Cu is reactive to oxygen molecules while graphene grains still retain certain structural integrity in order to keep the throttling effect.

In summary, we realize a direct identification of multilayer graphene stacks on Cu by optical microscopy after a combined treatment of UV exposure and ambient-condition heating. The sharp optical contrast, originating from the variation in copper oxide thickness underneath graphene grains, reproduces the stacking geometry with high fidelity to SEM images of pristine samples, demonstrating the correspondence among the optical contrast, the copper oxide thickness variation and the number of adlayers. The close correlation roots in the throttling effect of graphene grain with discrete structural defects in controlling the rate-determined oxidizing

agent supply. Room temperature UV exposure in air is a facile and easily available method to mildly induce vacancies into graphene grains without causing structure destruction, which further forms oxygen-transportation channels, given enough UV/O(^{3}P) pre-treatment. A following ambient condition heating treatment is necessary to enhance optical contrast so as to visualize pentalayer graphene stack on Cu. Copper oxide almost instantaneously forms at elevated temperatures when oxygen molecule reaches Cu surface by diffusing through the UV-generated vacancy channels in stack graphene adlayers. Fewer channels are available in thicker graphene layers, rendering differential oxygen supply and consequently variation in copper oxide thickness. This approach is simple and inexpensive. We believe that it can enable large-scale evaluation of CVD-derived graphene quality, which will be critical for optimizing CVD processing parameters of graphene growth for potential industrial application.

METHODS

Synthesis of Graphene on Cu by CVD method

An oxygen-assisted low pressure (LP-) CVD process was used to grow graphene on Cu foils.[14] A piece of commercially available Cu foil (25-μm-thick, #46365, Alfa Aesar China Chemical Co., Ltd.) was loaded into a quartz chamber and the temperature was increased to and maintained at 1060 ºC for 140 min in an atmosphere of H_2. Then oxygen gas with a flow rate of 1 standard-state cubic centimeter per minute (sccm) was introduced for 10min to passivate the Cu active sites for graphene nucleation.[14] For graphene growth, 0.3 sccm CH_4 and 200 sccm H_2 was employed and the growth time was typically 60 min.

Graphene adlayer visualization on Cu

As-grown graphene on Cu was placed into a UV/Ozone cleaner (Shanghai SunMonde Co., Ltd.) equipped with a low-pressure Hg light (power output of 20 $\mu W \cdot m^{-2}$, majority light at a wavelength of 254 nm, approximately 10% of light at a wavelength of 185 nm), whose inside treating environment has an operating temperature of ~60 ºC and humidity of ~16%, measured by a hydro-thermometer placed inside the device. Typical UV treatment time ranges from 30 min to 4 hours, depending on the layer number that needs to be visualized. After UV, the graphene sample was then placed on a hot plate and heated at 300 ºC in air for 5 s to several minutes.

Characterizations of graphene on Cu

The characterizations graphene adlayer visualization were carried out by scanning electron microscopy (SEM, 3 kV, S-3400, Hitachi Co., Ltd.), micro-Raman spectroscopy (532 nm wavelength excitation laser, LabRAM HR Evolution, Horiba Co., Ltd.), atomic force microscopy (tapping-mode, Veeco 3100 SPM, Shenzhen Haoguang Technology Co., Ltd.), and optical microscopy (yellow light by Shanghai 8XB-PC from Shanghai Optical Instrument Factory, and blue light by Olympus BXFM-ILHS from Olympus Co., Ltd).

Acknowledgement

Part of this work was financially supported by the National Science Foundation of China (11502231, 11321202, 11322219, 61471317), National Program for Special Support of Top-Notch Young Professionals, Zhejiang Provincial Natural Science Foundation of China (LQ15A020001) and the National Key Scientific Instruments and Equipment Development Project of China (61427901). We also acknowledge Mr. Guoxin Chen and Prof. Cheng-Te Lin from Ningbo Institute of Industrial Technology, CAS for the AFM measurements.

Author contributions

H.W. and P.Z. directed the research work, P.Z. and Y.C. designed the experiments, Y.C. conducted the experiments and measurements, D.Z. and Y.S. synthesized the materials, X.Z. transferred the materials, P.W., M.W. and S. Maruyama helped explain and discuss the results, Y.X. guided and coordinated the project, Y.C., P.Z. and H.W. analyzed the data, interpreted the results and wrote the text.

Additional information

Supplementary Information accompanies this paper at

http://www.nature.com/naturecommunications

Competing financial interests: The authors declare no competing financial interests.

REFERENCES

1. Lee, C.; Wei, X.; Kysar, J. W.; Hone, J., Measurement of the Elastic Properties and Intrinsic Strength of Monolayer Graphene. *Science* **2008,** *321* (5887), 385−388.

2. Castro Neto, A. H.; Guinea, F.; Peres, N. M. R.; Novoselov, K. S.; Geim, A. K., The electronic properties of graphene. *Rev. Mod. Phy.* **2009,** *81* (1), 109−162.

3. Novoselov, K. S.; Falko, V. I.; Colombo, L.; Gellert, P. R.; Schwab, M. G.; Kim, K., A roadmap for graphene. *Nature* **2012,** *490* (7419), 192−200.

4. Chen, S.; Wu, Q.; Mishra, C.; Kang, J.; Zhang, H.; Cho, K.; Cai, W.; Balandin, A. A.; Ruoff, R. S., Thermal conductivity of isotopically modified graphene. *Nat. Mater.* **2012,** *11* (3), 203−207.

5. Berger, C.; Song, Z.; Li, X.; Wu, X.; Brown, N.; Naud, C.; Mayou, D.; Li, T.; Hass, J.; Marchenkov, A. N.; Conrad, E. H.; First, P. N.; de Heer, W. A., Electronic Confinement and Coherence in Patterned Epitaxial Graphene. *Science* **2006,** *312* (5777), 1191−1196.

6. Stankovich, S.; Dikin, D. A.; Piner, R. D.; Kohlhaas, K. A.; Kleinhammes, A.; Jia, Y.; Wu, Y.; Nguyen, S. T.; Ruoff, R. S., Synthesis of graphene-based nanosheets via chemical reduction of exfoliated graphite oxide. *Carbon* **2007,** *45* (7), 1558−1565.

7. Li, X.; Cai, W.; An, J.; Kim, S.; Nah, J.; Yang, D.; Piner, R.; Velamakanni, A.; Jung, I.; Tutuc, E.; Banerjee, S. K.; Colombo, L.; Ruoff, R. S., Large-Area Synthesis of High-Quality and Uniform Graphene Films on Copper Foils. *Science* **2009,** *324* (5932), 1312−1314.

8. Kim, K. S.; Zhao, Y.; Jang, H.; Lee, S. Y.; Kim, J. M.; Kim, K. S.; Ahn, J.-H.; Kim, P.; Choi, J.-Y.; Hong, B. H., Large-scale pattern growth of graphene films for stretchable transparent electrodes. *Nature* **2009,** *457* (7230), 706−710.

9. Reina, A.; Jia, X.; Ho, J.; Nezich, D.; Son, H.; Bulovic, V.; Dresselhaus, M. S.; Kong, J., Large Area, Few-Layer Graphene Films on Arbitrary Substrates by Chemical Vapor Deposition. *Nano Lett.* **2009,** *9* (1), 30−35.

10. Gao, L.; Ren, W.; Xu, H.; Jin, L.; Wang, Z.; Ma, T.; Ma, L.-P.; Zhang, Z.; Fu, Q.; Peng, L.-M.; Bao, X.; Cheng, H.-M., Repeated growth and bubbling transfer of graphene with millimetre-size single-crystal grains using platinum. *Nat. Commun.* **2012,** *3*, 699.

11. Bae, S.; Kim, H.; Lee, Y.; Xu, X.; Park, J.-S.; Zheng, Y.; Balakrishnan, J.; Lei, T.; Ri Kim, H.; Song, Y. I.; Kim, Y.-J.; Kim, K. S.; Ozyilmaz, B.; Ahn, J.-H.; Hong, B. H.; Iijima, S., Roll-to-roll production of 30-inch graphene films for transparent electrodes. *Nat. Nanotechnol.* **2010,** *5* (8), 574−578.

12. Li, X.; Magnuson, C. W.; Venugopal, A.; Tromp, R. M.; Hannon, J. B.; Vogel, E. M.; Colombo, L.; Ruoff, R. S., Large-Area Graphene Single Crystals Grown by Low-Pressure Chemical Vapor Deposition of Methane on Copper. *J. Am. Chem. Soc.* **2011,** *133* (9), 2816−2819.

13. Sun, Z.; Raji, A.-R. O.; Zhu, Y.; Xiang, C.; Yan, Z.; Kittrell, C.; Samuel, E. L. G.; Tour, J. M., Large-Area Bernal-Stacked Bi-, Tri-, and Tetralayer Graphene. *ACS Nano* **2012,** *6* (11), 9790−9796.

14. Hao, Y.; Bharathi, M. S.; Wang, L.; Liu, Y.; Chen, H.; Nie, S.; Wang, X.; Chou, H.; Tan, C.; Fallahazad, B.; Ramanarayan, H.; Magnuson, C. W.; Tutuc, E.; Yakobson, B. I.; McCarty, K. F.; Zhang, Y.-W.; Kim, P.; Hone, J.; Colombo, L.; Ruoff, R. S., The Role of Surface Oxygen in the Growth of Large Single-Crystal Graphene on Copper. *Science* **2013,** *342* (6159), 720−723.

15. Zhao, P.; Kim, S.; Chen, X.; Einarsson, E.; Wang, M.; Song, Y.; Wang, H.; Chiashi, S.; Xiang, R.; Maruyama, S., Equilibrium Chemical Vapor Deposition Growth of Bernal-Stacked Bilayer Graphene. *ACS Nano* **2014,** *8* (11), 11631−11638.

16. Kim, H.; Mattevi, C.; Calvo, M. R.; Oberg, J. C.; Artiglia, L.; Agnoli, S.; Hirjibehedin, C. F.; Chhowalla, M.; Saiz, E., Activation Energy Paths for Graphene Nucleation and Growth on Cu. *ACS Nano* **2012,** *6* (4), 3614−3623.

17. Shu, H.; Tao, X.-M.; Ding, F., What are the active carbon species during graphene chemical vapor deposition growth? *Nanoscale* **2015,** *7* (5), 1627−1634.

18. Vlassiouk, I.; Regmi, M.; Fulvio, P.; Dai, S.; Datskos, P.; Eres, G.; Smirnov, S., Role of Hydrogen in Chemical Vapor Deposition Growth of Large Single-Crystal Graphene. *ACS Nano* **2011,** *5* (7), 6069−6076.

19. Zhang, X.; Wang, L.; Xin, J.; Yakobson, B. I.; Ding, F., Role of Hydrogen in Graphene Chemical Vapor Deposition Growth on a Copper Surface. *J. Am. Chem. Soc.* **2014,** *136* (8), 3040−3047.

20. Han, G. H.; Güneş, F.; Bae, J. J.; Kim, E. S.; Chae, S. J.; Shin, H.-J.; Choi, J.-Y.; Pribat, D.; Lee, Y. H., Influence of Copper Morphology in Forming Nucleation Seeds for Graphene Growth. *Nano Lett.* **2011,** *11* (10), 4144−4148.

21. Zhao, P.; Kumamoto, A.; Kim, S.; Chen, X.; Hou, B.; Chiashi, S.; Einarsson, E.; Ikuhara, Y.; Maruyama, S., Self−Limiting Chemical Vapor Deposition Growth of Monolayer Graphene from Ethanol. *J. Phys. Chem. C* **2013,** *117* (20), 10755−10763.

22. Blake, P.; Hill, E. W.; Castro Neto, A. H.; Novoselov, K. S.; Jiang, D.; Yang, R.; Booth, T. J.; Geim, A. K., Making graphene visible. *Appl. Phys. Lett.* **2007,** *91* (6), 063124.

23. Li, X.; Zhu, Y.; Cai, W.; Borysiak, M.; Han, B.; Chen, D.; Piner, R. D.; Colombo, L.; Ruoff, R. S., Transfer of Large-Area Graphene Films for High-Performance Transparent Conductive Electrodes. *Nano Lett.* **2009,** *9* (12), 4359−4363.

24. Song, J.; Kam, F.-Y.; Png, R.-Q.; Seah, W.-L.; Zhuo, J.-M.; Lim, G.-K.; Ho, P. K. H.; Chua, L.-L., A general method for transferring graphene onto soft surfaces. *Nat. Nanotechnol.* **2013,** *8* (5), 356−362.

25. Duong, D. L.; Han, G. H.; Lee, S. M.; Gunes, F.; Kim, E. S.; Kim, S. T.; Kim, H.; Ta, Q. H.; So, K. P.; Yoon, S. J.; Chae, S. J.; Jo, Y. W.; Park, M. H.; Chae, S. H.; Lim, S. C.; Choi, J. Y.; Lee, Y. H., Probing graphene grain boundaries with optical microscopy. *Nature* **2012,** *490* (7419), 235−239.

26. Gan, L.; Zhang, H.; Wu, R.; Ding, Y.; Sheng, P.; Luo, Z., Controlled removal of monolayers for bilayer graphene preparation and visualization. *RSC Adv.* **2015,** *5* (32), 25471−25476.

27. Novoselov, K. S.; Geim, A. K.; Morozov, S. V.; Jiang, D.; Zhang, Y.; Dubonos, S. V.; Grigorieva, I. V.; Firsov, A. A., Electric Field Effect in Atomically Thin Carbon Films. *Science* **2004,** *306* (5696), 666−669.

28. Derin, H.; Kantarli, K., Optical characterization of thin thermal oxide films on copper by ellipsometry. *Appl. Phys. A.* **2002,** *75* (3), 391−395.

29. Ferrari, A. C.; Meyer, J. C.; Scardaci, V.; Casiraghi, C.; Lazzeri, M.; Mauri, F.; Piscanec, S.; Jiang, D.; Novoselov, K. S.; Roth, S.; Geim, A. K., Raman Spectrum of Graphene and Graphene Layers. *Phys. Rev. Lett.* **2006,** *97* (18), 187401.

30. Sutter, P.; Sadowski, J. T.; Sutter, E. A., Chemistry under Cover: Tuning Metal−Graphene Interaction by Reactive Intercalation. *J. Am. Chem. Soc.* **2010,** *132* (23), 8175−8179.

31. Cheng, Y. C.; Kaloni, T. P.; Zhu, Z. Y.; Schwingenschlögl, U., Oxidation of graphene in ozone under ultraviolet light. *Appl. Phys. Lett.* **2012,** *101* (7), 073110.

32. Rhodin, T. N., Low Temperature Oxidation of Copper. II. Reaction Rate Anisotropy1. *J. Am. Chem. Soc.* **1951,** *73* (7), 3143−3146.

33. Huh, S.; Park, J.; Kim, Y. S.; Kim, K. S.; Hong, B. H.; Nam, J.-M., UV/Ozone-Oxidized Large-Scale Graphene Platform with Large Chemical Enhancement in Surface-Enhanced Raman Scattering. *ACS Nano* **2011,** *5* (12), 9799−9806.

34. Mulyana, Y.; Uenuma, M.; Ishikawa, Y.; Uraoka, Y., Reversible Oxidation of Graphene Through Ultraviolet/Ozone Treatment and Its Nonthermal Reduction through Ultraviolet Irradiation. *J. Phys. Chem. C* **2014,** *118* (47), 27372−27381.

Figure Legends

Figure 1. Visualization of graphene adlayers on Cu by OM after treated with UV light and heating. (a) Schematic of the oxidation treatments. The graphene/Cu sample was treated by UV light followed by heating in air. Pristine graphene is shown with slight color contrast for clarity. (b) Optical image of graphene/Cu sample after the UV/heating oxidation treatments. Different patterns appear and can be later confirmed as different graphene adlayers. (c) SEM image of the graphene adlayers observed in same area as shown in (b).

Figure 2. OM and SEM images of graphene single crystals and their adlayers after different UV treatment periods but the same heating time of 30 s. The upper OM image and lower SEM image in each panel are observed from the same graphene grain, and the inset in each image is an enlarged image of the boxed area for the center part of the graphene grain. (a−c) OM images of graphene adlayers with UV treatments of 60 min, 120 min, and 150 min, respectively, all of which are followed by heating in air at 300 ºC for 30 s. (d-f) Corresponding images of the same graphene adlayers in (a-c) when observed by SEM.

Figure 3. Influence of UV treatment and heating on the graphene adlayer visualization with different layer numbers. (a−c) OM images of graphene adlayers treated by UV light with different time of 60 min, 120 min, and 150 min, respectively. (d−f) OM images of the same graphene grains shown in (a-c) but with an additional heating for 30 s. (g) The relation between the visualized adlayer layer number and the time of UV treatment and heating.

Figure 4. (a) AFM image of an oxidized graphene grain on Cu surface after the UV treatment and heating. The corresponding height profile for the dotted line across the grain in the AFM image is shown in the right. (b, c) OM images of an oxidized graphene grain on Cu surface when observed with yellow and blue light, respectively. (d) OM image of a UV- and heating-treated graphene grain after reduced by acetic acid for 10 min. (e) OM image of the same graphene sample in (d) but with a re-oxidation of heating for 30 s.

Figure 5. Raman spectra of graphene samples with different treatments. All the measurements were conducted after transferring the treated samples onto SiO_2/Si substrates. The transferring process is conducted using a standard PMMA-assisted Cu-etching method, as described in the method section. (a) Pristine graphene sample without any treatment. (b) Graphene sample only treated with UV light for 180 min. (c) Graphene sample treated with UV light for 180 min followed by heating for 30 s. (d) Graphene sample only treated with heating for 30 s. (e, f) Schematic of the heating and UV treatments to graphene, respectively.

Figure 6. Schematic of the mechanism for the layer-by-layer visualization of graphene adlayers using UV treatment and ambient-condition heating. (i) Pristine CVD-derived graphene on Cu. (ii) UV-generated $O(^3P)$ is adsorbed onto graphene and the uncovered Cu surface is oxidized. (iii) Vacancies appear in graphene and Cu_xO thin film with varying thickness is formed beneath different graphene stacks with prolonged UV exposure. (iv) Additional ambient-condition heating treatment leads to more defects in graphene for thicker Cu_xO film with sharp contrast.

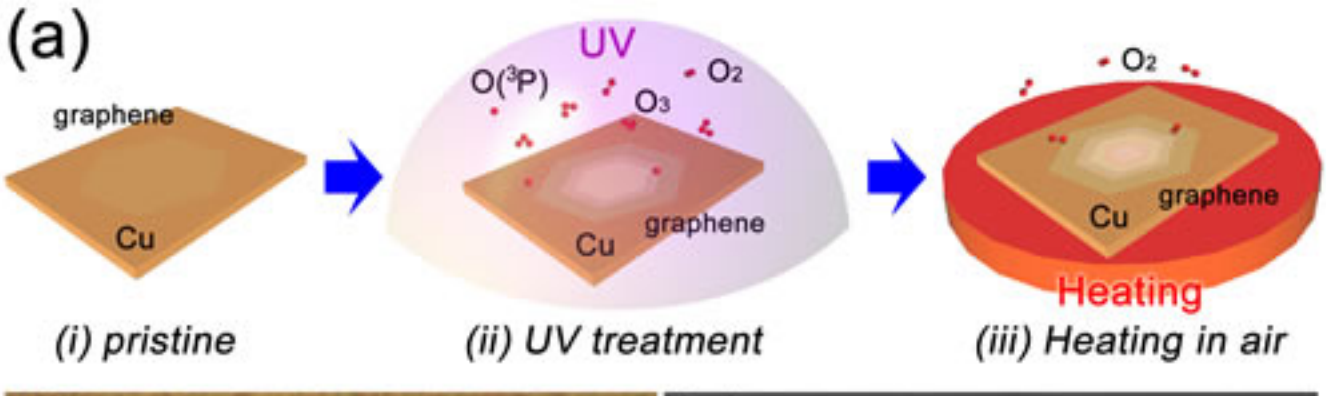

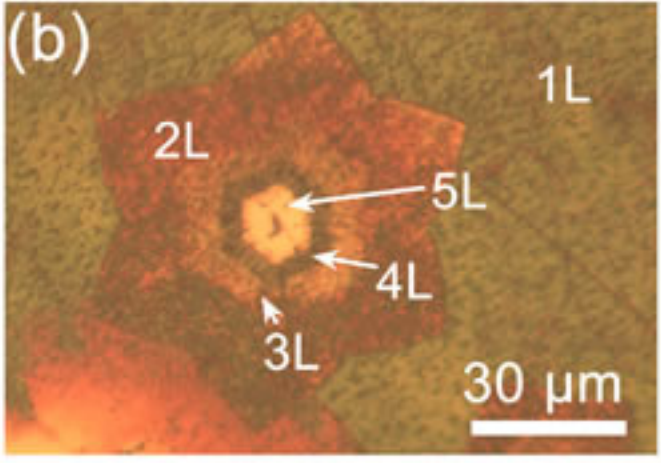

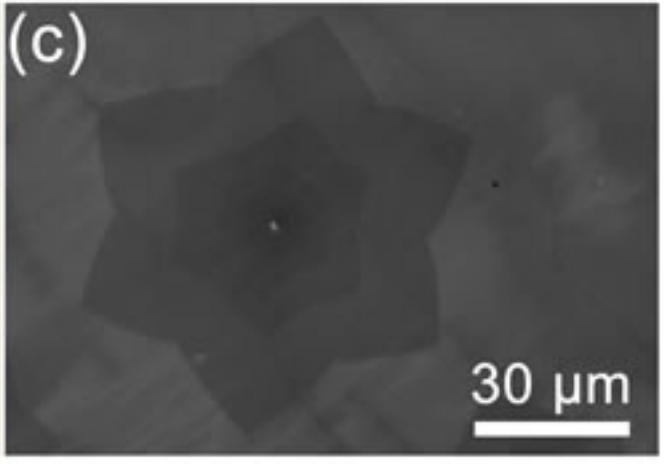

Figure-1 (Zhao)

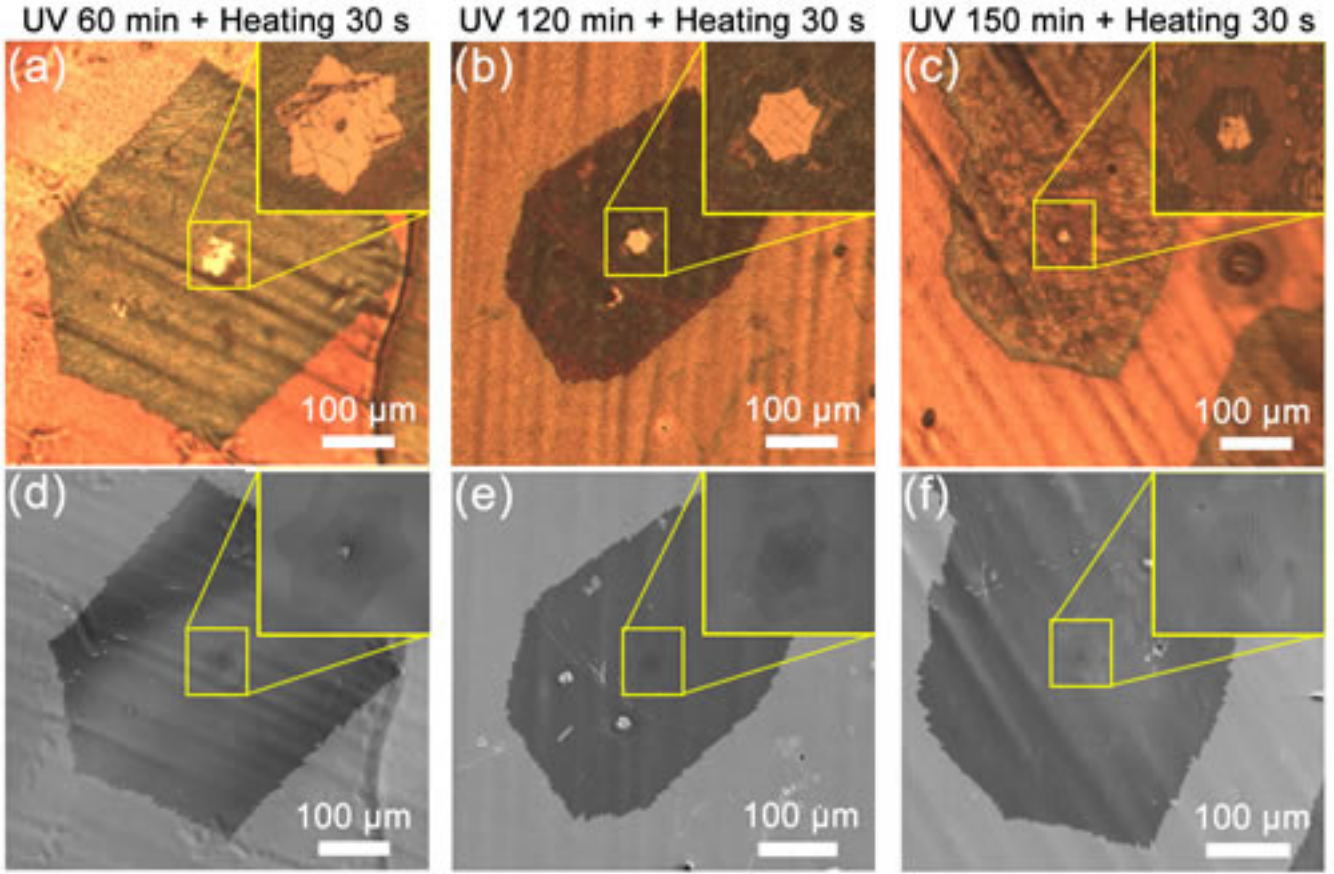

Figure-2 (Zhao)

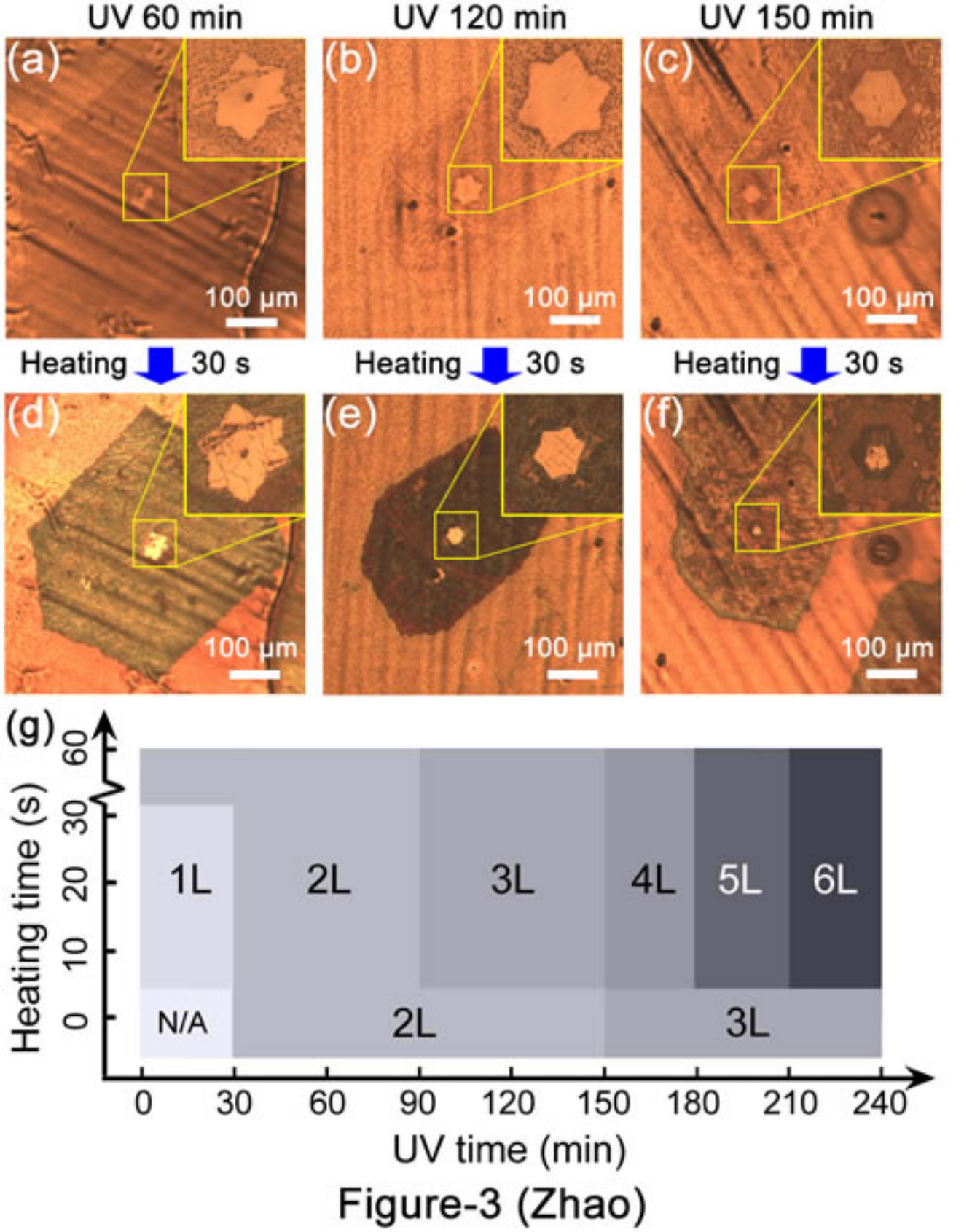

Figure-3 (Zhao)

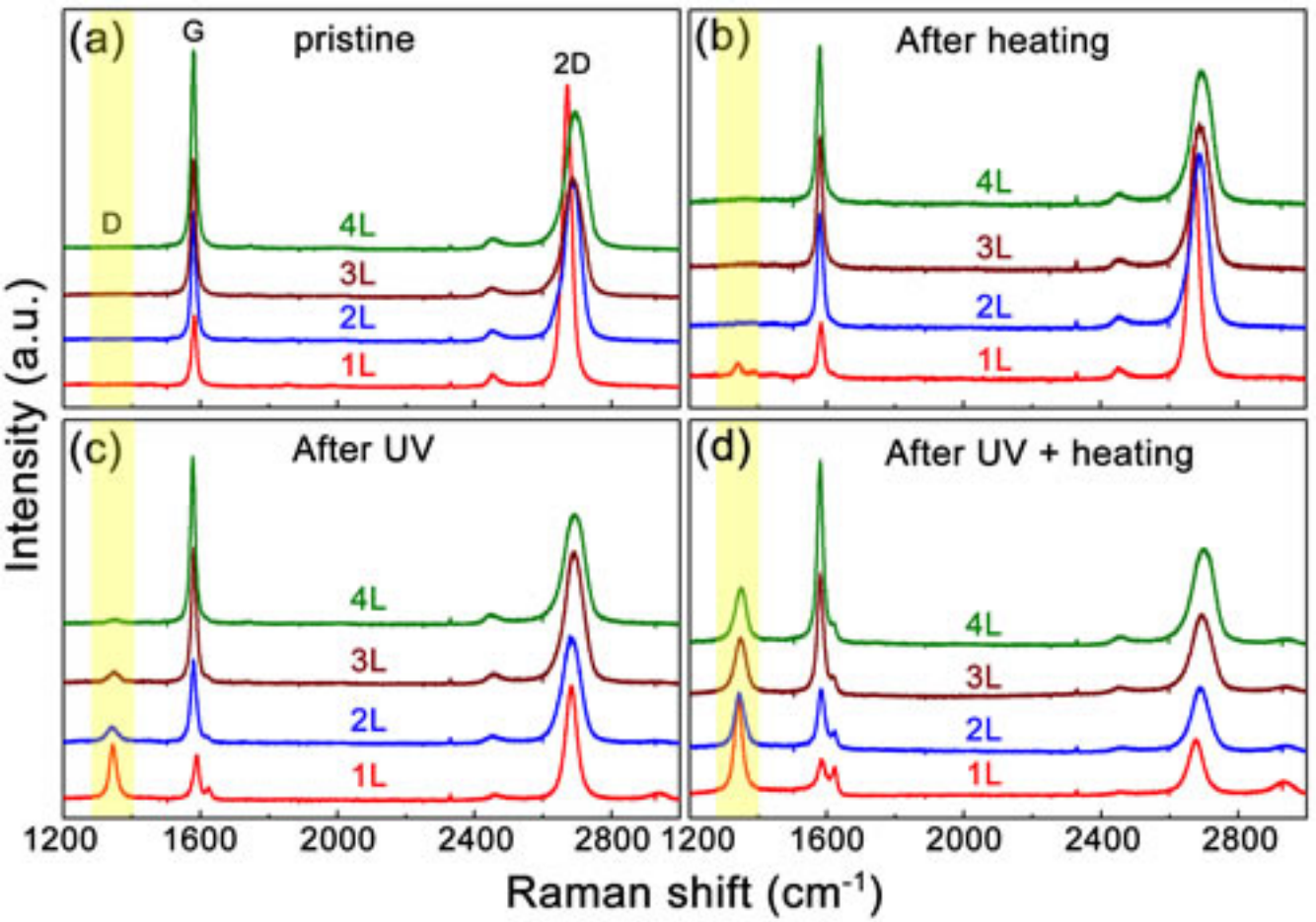

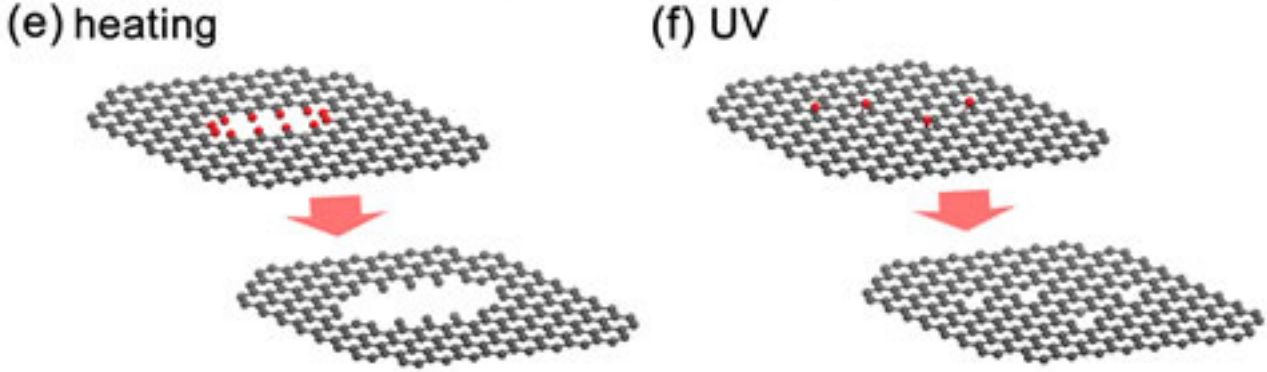

Figure-4 (Zhao)

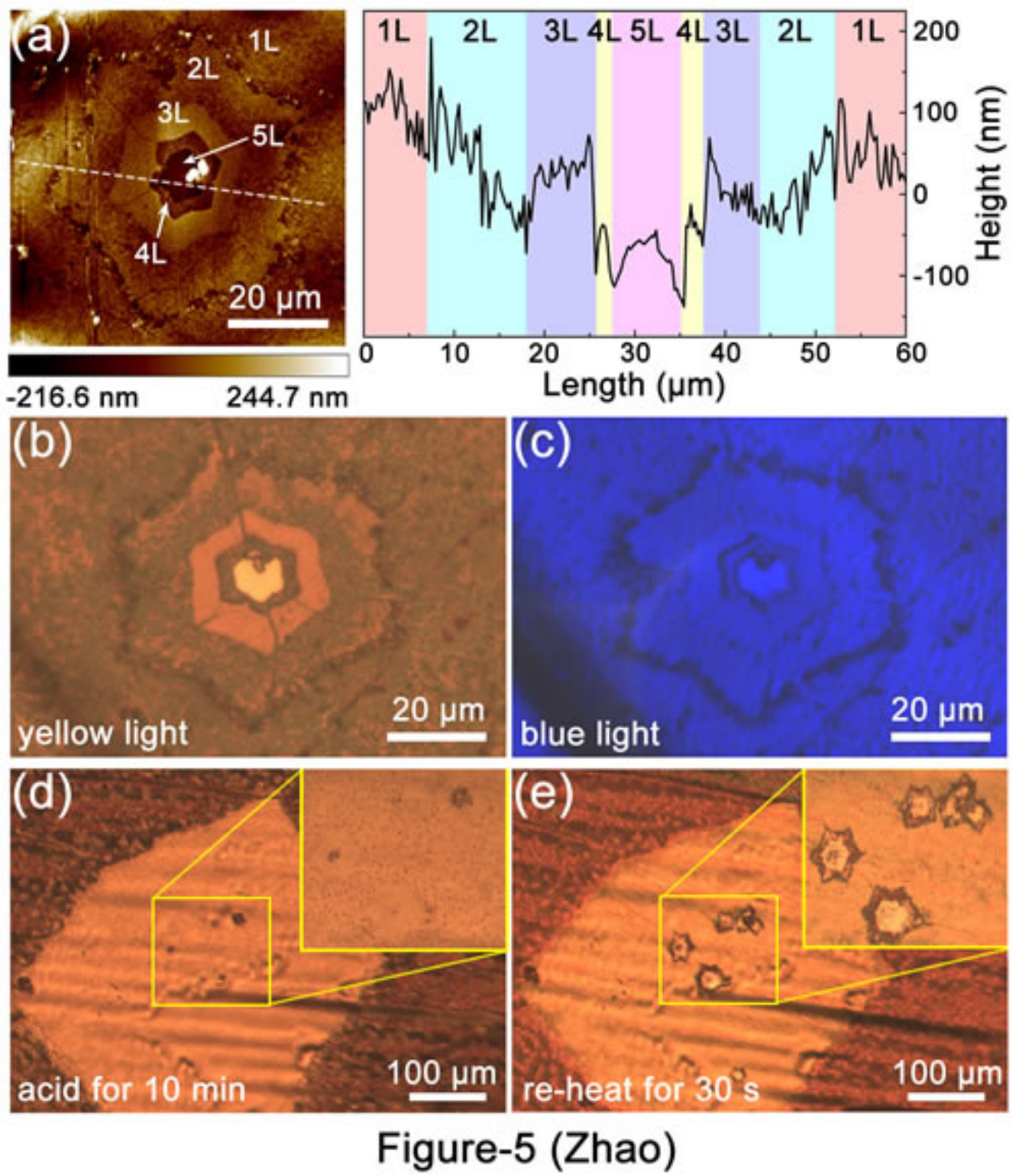

Figure-5 (Zhao)

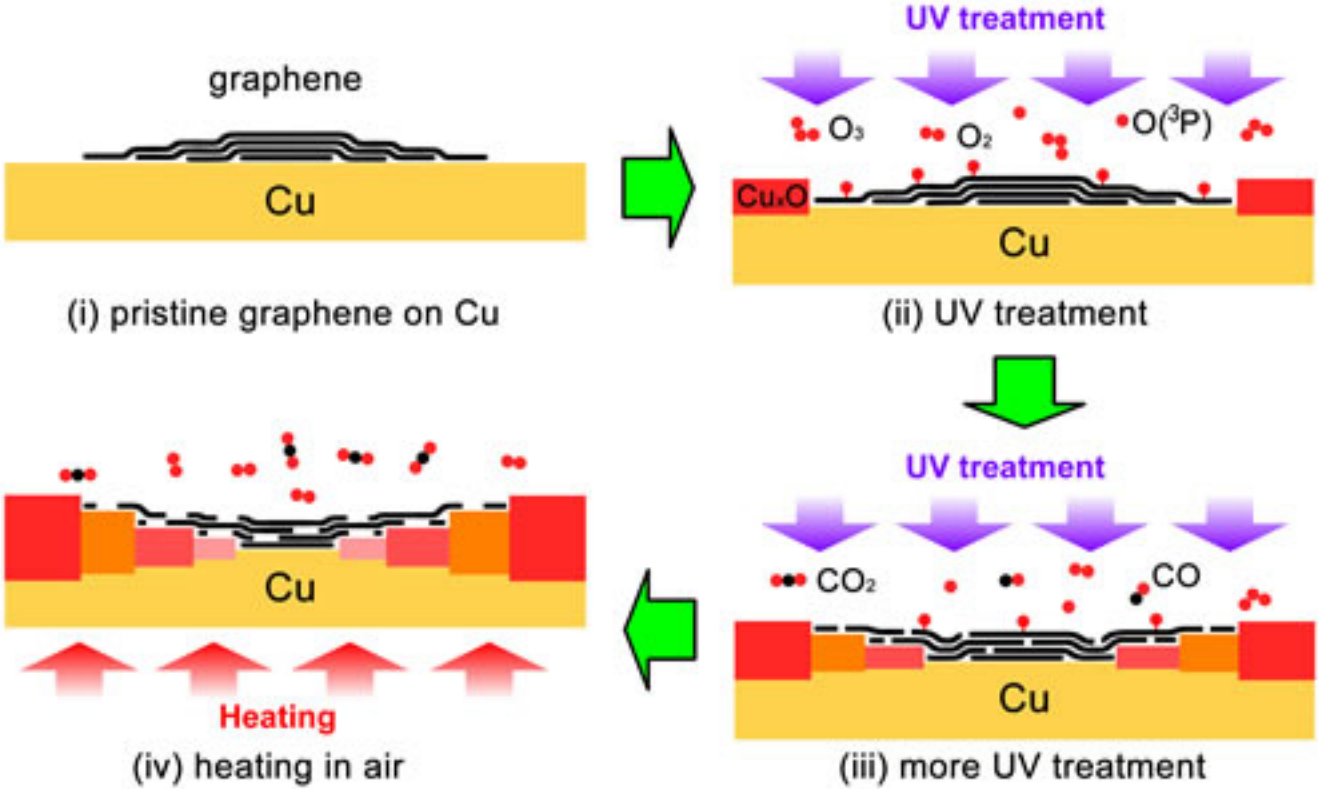

Figure-6 (Zhao)